TOWARDS A MORE REALISTIC PICTURE OF IN SITU BIOCIDE ACTIONS: COMBINING PHYSIOLOGICAL AND MICROSCOPY TECHNIQUES

SPERANZA M. [a,*], WIERZCHOS J. [a], DE LOS RIOS A. [a], PEREZ-ORTEGA S. [a], SOUZA-EGIPSY V. [b], ASCASO C. [a,*]

[a] Museo Nacional de Ciencias Naturales, MNCN-CSIC, Serrano 115 bis, 28006 Madrid, Spain

[b] Instituto de Ciencias Agrarias, ICA-CSIC, Serrano 115 bis, 28006 Madrid, Spain

Mailing address: Dept. de Biología Ambiental, Museo Nacional de Ciencias Naturales, Consejo Superior de Investigaciones Científicas (MNCN-CSIC), Serrano 115 bis, 28006 Madrid, Spain

*_Corresponding authors:_ Tel.: +34 917 452 500 ext.: 981010 and 980511 fax: +34 915 640 800.

E-mail addresses: speranzamariela@gmail.com (Mariela Speranza), ascaso@mncn.csic.es (Carmen Ascaso).

Abstract

In this study, we combined chlorophyll a fluorescence (ChlaF) measurements, using pulse-amplitude-modulate (PAM) equipment, with scanning electron microscopy in backscattered electron mode (SEM-BSE) and transmission electron microscopy (TEM) images to evaluate the actions of Koretrel at lower concentrations on *Verrucaria nigrescens* colonising a dolostone. ChlaF measurements are good indicators of the damaging effects of biocides. However, these indicators only provide an incomplete view of the mechanism of biocides used to control biodeterioration agents. The death of the *V. nigrescens* photobiont at two biocide concentrations was revealed by PAM, SEM-BSE and TEM. Once Koretrel was applied, the Fv/Fm ratios markedly fell in the first few hours after the 1.5% treatment, and ratios for the 3% dilution remained close to zero throughout the study. The algal zone shows the plasmolysed appearance of the photobiont cells, and important aspects related to the action of the biocide on free and lichenised fungi were also detected using SEM-BSE. Many of the mycobiont cells had only their cell walls preserved; although, some fungal hyphae in lichen thalli and some microorganisms in endolithic clusters maintained lipid storage in their cytoplasm. These results indicated that the combination of physiological and microscopy techniques improves the assessment of biocide action *in situ* and this will help to optimize protocols in order to reduce the emission of these compounds to the environment.

Keywords:

Biocide, Biodeterioration, Chlorophyll *a* fluorescence, Fungi, Lichen, Microorganisms, Ultrastructure, EM

1. Introduction

To control the biodeterioration of our cultural heritage buildings by organisms and microorganisms, it is necessary to apply treatments, including mechanical, physical and chemical, that are designed to inhibit biological growth (Berti et al., 2008; Caneva et al., 2008; Charola et al., 2011). The biocidal effects of these treatments in both the short and especially the long term need to be determined in addition to their potential interactions with the substrate to assess the effectiveness of such methods. A recent study has assessed the efficacy of laser treatment, a physical method, under laboratory conditions to control lichens and microorganisms from the same dolostone quarry used in the present experiments (Speranza et al., 2012).

To examine the biodeterioration of stone and the effects of biocides on microorganisms, a series of tests, or techniques, able to provide a precise diagnosis must be developed so that the biocidic actions on the microorganisms can be determined without removing them from their stone substrate, in a non-disturbed microecosystems.

Chlorophyll *a* Fluorescence (Chl*a*F) detection is a widespread technique used to assess the photosynthetic performance of lichen photobionts and plants (Baker, 2008; Schroeter et al., 1999; Tretiach et al., 2007). Using this tool, the efficacy of Koretrel to control lichen phototrophic epilithic microorganisms has been demonstrated both in the field and under laboratory conditions (Tretiach et al., 2010; Tretiach et al., 2007). Fluorescence parameters, minimal (Fo) or maximal (Fm) fluorescence and photosystem II (PSII) potential quantum yield (Fv/Fm) are influenced by environmental factors (Baruffo and Tretiach, 2007). Moreover, it seems that for lichens, both Fo and Fm are sensitive to temperature and to the instrument settings

(Nayaka et al., 2009). Additionally, intrathallus photosynthetic Chl*a*F variations have been observed in foliose lichens (Baruffo et al., 2008).

Imaging techniques such as scanning electron microscopy in backscattered electron mode (SEM-BSE) allow determination of the receptivity of the stone and deterioration state (Ascaso et al., 2002; Cámara et al., 2008; De los Ríos and Ascaso, 2005; De los Ríos et al., 2004; Miller et al., 2012). It is possible to observe free-living algae and fungi, lichen thalli and cyanobacterial and bacterial colonies and to assess the biogeomechanical and biogeochemical processes associated with the actions of the epilithic and endolithic microbiota. This type of study combined with molecular biology techniques has served to identify isolated fungi as the main colonising heterotrophic microorganisms of lithic substrates (Cámara et al., 2008; De los Ríos et al., 2009). The microhabitat occupied by cyanobacteria has been examined using the SEM-BSE technique, revealing the important deteriorating actions of these phototrophs and also identifying Preventol (alkyl-dimethyl-benzylamine chloride and isopropanol mixture) as the biocide that produces the most deleterious effects on the microbiota (Ascaso et al., 2002; De los Ríos and Ascaso, 2005).

The aim of this study was to combine the use of pulse amplitude modulation (PAM) Chl*a*F measurements carried out in the field with SEM-BSE images from collected lichen thalli, without separating it from its' substrate, thus providing a more complete picture of the effect of the biocide Koretrel on the primary lithic biodeterioration agents. Fluorescence variables provide diagnostic information concerning the effects on the photosynthetic function of the algal symbiont, whereas by using SEM-BSE tools, we can observe the effects produced on the cell ultrastructure in both symbionts and also on endolithic microorganisms. This study examined the use of a biocide, Koretrel, whose efficacy has already been established against other lichen

species, both *in situ*, in the laboratory, and on UNESCO World Heritage monuments (Penh, 2008; Smithsonian, 2012; Tretiach et al., 2010; Tretiach et al., 2007; Uchida et al., 2000).

2. Material and methods

2.1 Field experiments

Fieldwork was conducted on dolostone rocks from the Redueña quarry (917 m above sea level; N 40° 47.66´; W 3° 33.25´, Madrid, Spain). *Verrucaria nigrescens* Pers. is a widespread crustose epilithic lichen, with *Diplosphaera* sp. as the photobiont (Gueidan et al., 2011), that grows on limestone heritage buildings and monuments throughout Europe (Blazquez et al., 1995; Nimis and Martellos, 2010; Smith et al., 2010) and colonises extensive areas of a Cretaceous dolostone quarry face (Redueña, Madrid) (Figs. 1A-B). From Roman times to the mid-twentieth century, stone from this quarry has been used in the construction of monuments, some of which currently form part of central Spain's cultural heritage.

Microclimate data such as atmospheric relative humidity (RH) and air temperature (T) were recorded beginning one month before the onset of treatment (from 10th October to 13th December of 2010) to determine the microclimate conditions in the area inhabited by the lichens using RH/T sensors with data logger U23Pro v2 (HOBO®; precision, ±2.5% RH/ ±0.2ºC). The data logger was set to take measurements every 30 minutes, and the sensor was shaded from the sun and positioned approximately 1.5 m above soil level. For the most part, the data collected overlapped with the time of the experiment (Fig. 1C). We conducted our experiments in late autumn because our Chl*a*F measurements (Fv/Fm) at the end of the summer indicated that the *V. nigrescens* thalli were metabolically inactive. Additionally, to avoid seasonal variation, the duration of the experiment was 28 days.

2.2 ChlaF measurements

To identify *V. nigrescens* thalli with active photobionts, Chl*a*F measurements were taken in the field described by Schroeter et al. (1992) and a few days before the biocide was applied, as described by Baruffo and Tretiach (2007). To minimise intrathallus variation in Chl*a*F measurements, determinations were made in the same portion of the thallus. Due to the small thallus size of *V. nigrescens*, measurements were made at a single spot. We established three 30 × 30 cm plots on the quarry face occupied by *V. nigrescens* thalli and placed a numbered grid in each plot so that we could identify each lichen thallus (small thalli 2-3 cm) with a coordinate system (inset in Fig. 1B).

The PSII quantum yield (Fv/Fm = variable fluorescence/maximal fluorescence) is an indicator of lichen vitality and was determined using a PAM fluorometer (Mini PAM, Walz, GmbH, FRG) on fully hydrated, dark-adapted thalli (Maxwell and Johnson, 2000). The thalli were sprayed with distilled water to reactivate the photosynthetic system and then covered for 30 minutes with a double layer of dark-coloured velvet to induce dark-adaptation and ensure that all PSII reaction centres were open (Jensen, 2002). Chl*a*F measurements were taken by passing saturation light through a flexible optic fibre with an active diameter of 5.5 mm, positioned at 90° over the dark-adapted thallus surface. The fluorescence signal of the dark-adapted specimens (Fo) and the fluorescence signal obtained during the saturation pulse (Fm) were determined with an 800 ms saturation pulse of *ca.* 2500 µmol m^{-2} s^{-1} light intensity.

2.3. Biocide treatments in the field

Koretrel© (Tokai Concrete Co., Japan), a concentrated blend of alcohol alkylene oxide (97.56%), denatured alkyl trihydroxybenzene polyoxide (0.48%), alkylaminotriazine (0.98%) and *N'*-(3,4-dichlorophenyl)-*N*,*N*-dimethyl urea (0.98%), was kindly supplied by Prof. M. Tretiach (Trieste University, Italy).

Three plots were subjected to biocide treatment. Before treatment, the lichen thalli were moistened with a water spray, and Chl*a*F measurements (time 0) were repeated to confirm lichen vitality. Koretrel diluted in distilled water at two concentrations, 1.5% and 3%, was applied several times to the lichen surface with the aid of a brush at short time intervals (*ca.*10 min) until complete imbibition of the thalli. Ninety-two thalli were treated with 1.5% Koretrel, 117 were treated with 3% Koretrel solution, and 51 untreated thalli were used as controls. Field Chl*a*F measurements were performed at 4 hours and 1, 2, 4, 7, 14 and 28 days after biocide treatment. At 28 days, the thalli were removed using a soft metal brush.

2.4 Stereomicroscopy

Control and Koretrel-treated samples were observed using a Leica S8 APO stereomicroscope equipped with a Leica EC3 digital camera. The images were captured at different magnifications using LAS EZ software.

2.5 Electron microscopy

To determine the biocidal effects at the cell level, we examined the structure of the epilithic lichenised microorganisms as well as that of the microorganisms occurring in the endolithic zone before and after Koretrel treatment. Observations were also made after

mechanical cleaning of the quarry front surface at the end of the experiment (28 days) using scanning electron microscopy techniques.

2.5.1 Scanning electron microscopy in backscattered electron mode (SEM-BSE)

Control and Koretrel-treated stone samples (three samples per treatment) colonised by lichens and microorganisms as well as samples collected after mechanical treatment were processed for SEM-BSE observation according to the method developed by Wierzchos and Ascaso (1994). Briefly, small (a few cm^3) blocks of lichen thalli were collected without separating them from their substrate and carefully cut with a diamond saw in the transverse direction of the stone samples. The samples with *V. nigrescens* bearing endolithic microorganisms were fixed in 3% glutaraldehyde in 0.1 M cacodilate buffer and then in a secondary fixative using a 1% OsO_4 solution in 0.05 M cacodilate buffer. After fixing, the samples were dehydrated in a series of ethanol solutions, embedded in LR White^{TM} resin and fine-polished after polymerisation. The fine-polished surfaces of the cross-sections were carbon coated and examined using a DMS 960 Zeiss SEM equipped with a four-diode, semiconductor BSE detector. The microscope operating conditions were as follows: 0º tilt angle, 35º X-ray take-off angle, 15 kV acceleration potential, 15 mm working distance and 1–5 nA specimen current range.

2.5.2. Transmission electron microscopy (TEM)

Control and treated *V. nigrescens* thalli were fixed, dehydrated and embedded in Spurr´s resin as described elsewhere (Ascaso and Galvan, 1976; De los Ríos and Ascaso, 2002). All samples were processed within two days of collection. Ultrathin sections were stained with lead citrate and observed using a Leo 910 transmission electron microscope.

3. Results

The relative humidity (RH) and temperature (T) are shown in Fig. 1C. The results on the left side of the arrow correspond to RH and T before biocide application, and those on the right side correspond to the biocide experiment. The microclimate data indicate high RH values, and for some days the RH even reached 100% of water vapour partial pressure (Fig. 1C).

Figure 2 provides the mean Fv/Fm values for the controls and different treatments recorded over the 28 days of the study. For the 51 control samples, mean Fv/Fm values ranged from 0.411 to 0.495, with a maximum value of 0.793 and minimum of 0.300. These Fv/Fm ratios were similar to those measured in the days preceding the quarry trial and to those determined in reactivated thalli in the laboratory. The mean fluorescence ratio for the 92 thalli treated with the 1.5% Koretrel solution was 0.515 (maximum 0.880, minimum 0.403) at the time of application, and this level subsequently decreased, from as early as four hours post-application, to a mean of zero, which persisted until the end of the study period when the ratio recorded was 0.036-0.046. The corresponding Fv/Fm ratios for the 3% Koretrel treatment (n=117) were 0.519 (range 0.431 to 0.621) upon treatment, and zero after four hours, with this value persisting until the end of the experiment. The mean value of Fv/Fm obtained for the control thalli at the study outset (November 16, 2010) was 0.490 and this value dropped to 0.468 four hours later. The maximal and minimal Fv/Fm values for the control thalli also diminished slightly after four hours. The Fv/Fm continued to fall over the following two days, rising on days 3 and 4 and then persisted until the end of the 28-day period.

SEM-BSE images of the lichen thallus-rock complex allowed the observation of the discrete areoles of the healthy crustose thallus without treatment (white open arrows, Fig. 3A). In

Fig. 3B, the damage to the substrate produced by the thallus was clear, as the extent of hyphal penetration in the substrate can be seen (black dotted arrows). In addition, it was observed that these hyphae enveloped minerals, which became trapped and microdivided (asterisks Fig. 3B). The depth of hyphal penetration in the stone was approximately 0.2 mm. Figure 3C shows a detailed view of the algae and fungi within the thallus. These fungal cells showed high lipid contents localised in lipid bodies. The top of Fig. 3D shows lichen thalli, and the middle zone shows cell clusters in endolithic zones of the substrate 0.2-0.5 mm beneath the surface. The inset for Fig. 3D provides a detailed image of the cluster of algal and fungal cells. The good ultrastructural appearance of the algal cells observed by SEM-BSE in the *V. nigrescens* thallus before biocide treatment was in close agreement with the Chl*a*F measurements obtained. According to both the microscopy and fluorescence data, the algae appeared to be in good condition, which also corresponded with the good ultrastructural state exhibited by the fungal cells.

The thalli treated with the 1.5% Koretrel solution showed very altered areolar structures and detachment from the substrate (Fig. 4A white open arrows). Many empty fungal cells were observed in the upper part of the thallus (Fig. 4B white open arrows). A detailed picture of the algal zone (Fig. 4C) showed the plasmolysed appearance of the photobiont cells as the plasma membrane was separated from the cell wall (white arrows). The fungal cells were also dead, and only some of them preserved their cell walls (black arrows in Fig. 4C). In some of the micrographs, the substrate-lichen thallus interface can be seen more clearly (Fig. 4D), and in some cases, the fungal cells of the thallus fully adhered to the rock still showed the appearance of cells rich in lipid bodies (Fig. 4D, white dotted arrows). Through TEM (Fig. 5), the ultrastructural appearance of the photobiont of *V. nigrescens* without biocide treatment was observed (Fig. 5A)

along with that of the photobiont following treatment with the 1.5% Koretrel solution (Fig. 5B). In the chloroplasts of the algae in Fig. 5A, we distinguished the thylakoids as well as the pyrenoglobuli. This is the normal appearance of the pyrenoids of many algae, with this structure occupying the centre of the chloroplast. Adjacent to the algal cell, a fungal cell is present. In the photobiont in Fig. 5B, the chloroplast structure has disappeared as the thylakoids vanished. Moreover, a mass formed from thylakoidal lipid remains was observed, and the pyrenoid, despite still occupying a central position in the cell, showed pyrenoglobuli that are difficult to distinguish. Thus, layers of thylakoids that are difficult to discern occur inside the pyrenoid, and the remains of the pyrenoglobuli appear aligned with these.

The micrographs showing the effects of the 3% Koretrel treatment revealed its' profound attack on thalli and the endolithic microbiota as may be seen in Fig. 6A. This figure shows that the lichen thallus has not taken up the fixatives (low signal in BSE) used to prepare the samples for SEM-BSE, which indicated that all cells, both photobiont and mycobiont, were dead. This may be observed in more detail in Fig. 6B. In all thalli, the same effects as those of the 1.5% Koretrel treatment were produced in the algal and fungal cells but to a greater degree, and all observations indicated cell death. In addition, the hyphae of the lower thallus zone lacked the lipid bodies observed in response to this concentration of the biocide, and these appeared empty or without a trace of lipids in their cytoplasm (Fig. 6C). The photobiont layer and the mycobiont hyphae showed significant changes in their ultrastructure, including plasmolysis of all the cells and the inability to capture osmium tetroxide (Fig. 6C). Figure 6D shows an endolithic zone (a detail of Fig. 6A inset) where all hyphae were dead.

The zone treated with the Koretrel 3% solution during 28 days is shown in Fig. 7A. This image was obtained before mechanical cleaning. Mechanical cleaning (Fig. 7B) left a surface zone exposed where the remains of algae were left behind. These samples were subsequently processed for SEM-BSE observation. Figure 7C shows an SEM-BSE image of a section cut transverse to the surface of the rock as shown in Fig. 7B. This image shows that the algal-fungal cluster (which belongs to an endolithic colonisation that is not related to the epilithic *V. nigrescens* thalli) now appears much closer to the surface in response to brushing away the lichen remains (Fig. 7C). Some cells even appeared on the surface itself, which would explain the green colour of the exposed dolomite surface after cleaning. In Fig. 7C, some clusters had a normal appearance (black arrow and inset) while others were damaged (white arrow). In Fig. 7D, a detailed view of a cluster of algae and fungi is provided showing that some algal cells were not affected by the biocide (white arrows), and the fungal cells also appeared well preserved (black arrows). Thus, the biocide most likely partially reached this zone, and the mechanical cleaning procedure caused these algae-fungi associations to emerge.

Our SEM-BSE data revealed the mycobiont to be no less sensitive than the photobiont to the biocide; a 1.5% dilution of Koretrel induced damage to the epilithic thallus in both the photobiont and mycobiont (Fig. 4). Nevertheless, some mycobionts whose cytoplasms were filled with lipid bodies maintained these structures (Fig. 4D) and these cytoplasms were similar to those of the control (Figs. 3B-C), which showed numerous lipid bodies. In response to 3% Koretrel treatment, the SEM-BSE images showed that all the algal and fungal cells of the thallus were indisputably dead (Fig. 6). By comparing Figs. 6B and 3B, the damage produced by 3% Koretrel treatment to the cells of the *V. nigrescens* thallus can be clearly seen. SEM-BSE imaging also indicated that the 3% Koretrel solution affected the hyphae in the lower part of thallus to a

greater extent than the 1.5% Koretrel solution; the higher concentration of the biocide completely destroyed the lipid globules and also affected the endolithic hyphae some 0.2- 0.3 mm beneath the rock surface.

4. Discussion

In this study, we considered all seasonal effects that could influence fluorescence measurements (Baruffo and Tretiach, 2007), the intrathalline heterogeneity that could exist as observed in foliose lichens (Baruffo et al., 2008) and metabolic perturbations that could induce changes in Chl*a*F measurements as reported in vascular plants (Barbagallo, 2003). In our experiments, we have taken into account that lichens adapted to light are particularly resistant to photoinhibition when dehydrated and, furthermore, when humid they are more sensitive to high radiation (Kappen et al., 1998).

Microclimate measurements were taken beginning one month before the onset of the treatments and during the experiment to determine the conditions in the area inhabited by the lichens. The obtained RH values and the occurrence of some days with the RH reaching 100% of vapour water pressure meant that heavy fog or rainfall could have occurred prior to sample collection. These data and temperatures were typical of those generally recorded in November in central Spain.

The high RH that was recorded in the area could perhaps explain the mean starting yield of 0.490 that was recorded for the controls both at 0 hours and in the following hours, persisting until the second day when the yields stabilised. This baseline value of 0.490 for Fv/Fm is below the values obtained by Baruffo and Tretiach (2007), who recorded means of 0.771 to 0.625 between December 2003 and December 2004 in *Parmelia subrudecta* in southern Tuscany.

Taking into account the results of Nayaka et al. (2009), these differences could also be attributed to factors such as the thallus anatomy, thallus size and photobiont distribution and species.

Once Koretrel was applied, the Fv/Fm ratios markedly fell in the initial few hours. However, these ratios recovered slightly over the first 2 days for the 1.5% treatment, and ratios for the 3% dilution remained close to zero during the 28 days of the study. In an evaluation of the effects of three biocides on two endolithic lichens, *Acrocordia conoidea* and *Baglietoa marmorea*, as determined by Chl*a*F measurements acquired by PAM, Tretiach et al. (2010) described its excellent sensitivity to quantify PSII quantum yield variations undetectable through epifluorescence microscopy, and these authors observed Fv/Fm zeroing three hours after treatment with undiluted Koretrel and a reduced effect when the biocide was diluted. In the present study, in response to the 3% dilution of Koretrel, Fv/Fm zeroing occurred as early as four hours after treatment. In contrast, following the Koretrel 1.5% treatment, the Fv/Fm fell to 0.025 at four hours and fluctuated from 0.036 to 0.058 until the end of the study at 28 days.

According to Tretiach et al. (2010), Chl*a*F measurements are helpful in the field of stone conservation to standardise biocide application protocols. Pulsed amplitude modulation fluorometry is fortunately a non-destructive method, allowing for the study of large surfaces in short periods of time. However, Chl*a*F measurements in response to a biocide can vary and are only an indicator of the functionality of the photosynthetic apparatus of the algal symbiont. Thus, for a better diagnosis of biocide actions, impacts on the mycobiont should also be determined, whether epilithic or endolithic, as well as the effects on free-living fungi given their established destructive behaviour. It would seem that the diagnosis of the effects of biocides on these microorganisms *in situ* (SEM-BSE images from collected lichen thalli without separating it from

its substrate) can only be made using imaging techniques. Because microscopy procedures are destructive, it is best if samples can be obtained of fieldstones or quarry stones, though it is possible to acquire tiny fragments of stone from an historic building. Such observations provide real insight into the processes occurring in the symbiont as well as the remaining heterotrophic and phototrophic free-living microorganisms that are found on the surface or within the rock and contribute to its deterioration. In this case, the SEM-BSE images have shown the plasmolysis of the cells of the thallus in photobionts and mycobionts and for both treatments. We observed that lipid structures remained only in some hyphae located in the bottom of the thallus in the 1.5% Koretrel treatment. After application of the 3% Koretrel solution, plasmolysis was complete in all of the cells. In hyphae of the cortex only the walls were observed, and every cell that maintained cytoplasmic remains did not take up osmium tetroxide, which indicated that they were all dead without exception. For a better view of these events, algal and fungal cells were also studied by transmission electron microscopy (TEM).

Following Koretrel treatment, the thylakoid lamellae of the chloroplast were indistinguishable by TEM. Considering the important role played by these structures and that their largest particles may be associated with PSII and smallest particles with PSI (Arntzen et al., 1969; Rapsch and Ascaso, 1985), this observation of completely disrupted thylakoids and the Chl*a*F data obtained by PAM were perfectly consistent with the effects of the biocide. In addition to these effects on the thylakoids, any damage to the pyrenoid will be crucial because it has been shown that, as was demonstrated in lichens, this is the main storage site of ribulose-1,5-bisphosphate carboxylase oxygenase (Ascaso et al., 1995). In a study designed to examine the effects of different relative humidity conditions on the pyrenoid in response to conditions of dehydration (Brown et al., 1987), the matrix was disrupted and the pyrenoglobuli adopted a

peripheral location. In the present study, we observed that the typical structure of the pyrenoid matrix was absent after the biocide treatment, and the pyrenoglobuli, although not located peripherally, appeared blurred indicating the loss of their typical osmiophilic nature. While PAM cannot reveal what is happening to the pyrenoid, the images obtained of the pyrenoid provided more information about the biocide action on the photosynthesis in the treated thalli.

These observations of a damaged photobiont are in accordance with the previously reported effect of the Koretrel active ingredients that specifically interfere with the photosynthetic process at the level of plastoquinones, inhibiting the photosynthesis (Metz et al., 1986). These facts also indicated the highly lichenicidal action of Koretrel (Tretiach et al., 2010; Tretiach et al., 2007). Following 4 to 8 days of Koretrel treatment, Tretiach et al. (2010) observed the breakdown of the activity of PSII, a finding in line with the ultrastructural changes detected here in the lichen's photosynthetic cells.

The important role played by mycobionts and free fungi in the colonisation of stone has been widely established (Gadd, 2007; Gorbushina and Broughton, 2009). In some studies, biocides have been tested on isolated microbiota by cultivating the microorganisms in mortar blocks and applying the different biocides *in situ* (Gorbushina et al., 2003). In a recent investigation in which the mycobionts and photobionts of two endolithic lichens were isolated and inoculated on stones used to construct cultural heritage buildings, the mycobionts showed different modes of penetration while the algae lacked this ability (Favero-Longo et al., 2009). For these observations, the authors used light microscopy and SEM-BSE techniques, as in our study, and they suggested that such methods could be used to plan treatment strategies for the conservation of stone monuments.

The presence of clusters of algae and fungi in endolithic positions in the dolostones of abandoned quarry fronts was previously demonstrated using SEM-BSE (Cámara et al., 2011). In the present study, some algae-fungi clusters in the stone interior appeared to be less damaged by biocide treatment than algae and fungi from the lichen thalli (Figs. 7 C-D). In the study by Camara et al. (2011), SEM-BSE observations of endolithic colonisation were confirmed by denaturing gradient gel electrophoresis, and the efficacy of the treatments was measured after 4 and 16 months; it was noted that the effects on the endolithic communities were dependent on how efficiently and completely the rock surface had been previously cleaned. In our study, we unexpectedly confirmed the death of both the algal and fungal cells of the epilithic thallus after 28 days of Koretrel treatment while the SEM appearance of the endolithic algal-fungal clusters in control and treated samples sometimes were similar. At this point, we are unable to explain this finding unless Koretrel, like other biocides, has a limited capacity to penetrate the stone and cannot reach the spaces where these algal-fungal associations reside (Cámara et al., 2011; De los Ríos et al., 2012). It is possible that such associations could have implications for recolonisation of the stone.

5. Conclusions

The findings of some studies suggest that Chl*a*F measurements are good indicators of the damaging effects of biocides on different biodeterioration agents. However, as increasing evidence exists for the important role played by fungal hyphae in stone alteration processes, the use of techniques that only reflect the state of phototrophic microorganisms is likely to be limited. Our results indicated that, while there is still room for improvement, the combined use of Chl*a*F measurements and SEM-BSE imaging gave a more complete picture of the effects of a

given biocide on the main components of a microbial lithic community involved in biodeterioration processes. Using this approach, a better selection of an effective biocide could also be made to combat all microbial agents responsible for stone biodeterioration, which would facilitate the optimization of biocide application protocols, particularly the minimum effective biocide dose in order to reduce unnecessary emissions of these compounds into the environment.

Acknowledgments

This work was funded by Programa Geomateriales (CAM, S2009/Mat-1629) and CGL 2010-16004 and CTM 2009-12838-CO4-03 from MICINN. The authors thank F. Pinto from the Electron Microscopy Facility, ICA-CSIC (Madrid), and T. Carnota, M. Castillejo and J. M. Hontoria from the MNCN-CSIC (Madrid) for technical assistance. We also thank Prof. M. Tretiach (Trieste University, Italy) for making recommendations for field experiments. M. Vivas, Prof. Ana Pintado and Prof. L. García Sancho of the UCM (Complutense University of Madrid) were responsible for the M.S. training on PAM equipment. M.S. wishes to thank Prof. J. Delgado Rodriguez (Lab. Nacional de Engenharia Civil, Portugal) for training and helpful advice given in "Workshop nº 9 Tratamento e Monitorização da Colonização Biológica na Pedra" organised by the World Monuments Fund, Portugal.We also thank A. Burton for reviewing the English. M. Speranza and S. Pérez-Ortega are contract holders of the CSIC-JAE Fondo Social Europeo.

References

Arntzen CJ, Dilly RA, Crane FL. A comparison of chloroplast membrane surfaces visualized by freeze-etch and negative staining techniques: and ultrastructural characterization of membranes fractions obtained from digitonin treated spinach chloroplast. Journal of Cell Biology 1969; 43: 16-31.

Ascaso C, Galvan J. The ultrastructure of the symbionts of *Rhizocarpon geographicum*, *Parmelia conspersa* and *Umbilicaria pustulata* growing under dryness conditions. Protoplasma 1976; 87: 409-418.

Ascaso C, Valladares F, De losRios A. New ultrastructural aspects of pyrenoids of the lichen photobiont *Trebouxia* (Microthamniales, Chlorophyta). Journal of Phycology 1995; 31: 114-119.

Ascaso C, Wierzchos J, Souza-Egipsy V, De los Rios A, Delgado Rodrigues J. In situ evaluation of the biodeteriorating action of microorganisms and the efects of biocides on carbonate rock of the Jeronimos Monastery (Lisbon). International Biodeterioration & Biodegradation 2002; 49: 1-12.

Baker NR. Chlorophyll Fluorescence: A probe of Photosynthesis In Vitro. Annu. Rev. Plant Biol. 2008; 59: 89-113.

Barbagallo RP. Rapid, Noninvasive Screening for Perturbations of Metabolism and Plant Growth Using Chlorophyll Fluorescence Imaging. Plant Physiology 2003; 132: 485-493.

Baruffo L, Piccotto M, Tretiach M. Intrathalline variation of chlorophyll a fluorescence emission in the epiphytic lichen *Flavoparmelia caperata*. Bryologist 2008; 111: 455-462.

Baruffo L, Tretiach M. Seasonal variations of Fo, Fm, and Fv/Fm in an epiphytic population of the lichen *Punctelia subrudecta* (Nyl.) Krog. The Lichenologist 2007; 39: 555-565.

Berti S, Pinzari F, Tiano P. Control of Biodeterioration and Bioremediation Techniques. Physical Methods. In: Caneva G, Nugari MP, Salvadori O, editors. Plant Biology for Cultural Heritage. Biodeterioration and Conservation. Getty Publications, Los Angeles, 2008.

Blazquez F, Calvet F, Vendrellc M. Lichen alteration and mineralization in calcareous monuments of northeastern Spain. Geomicrobiology Journal 1995: 223-247.

Brown DH, Ascaso C, Rapsch S. Ultrastructural Changes in the Pyrenoid of the Lichen *Parmelia sulcata* stored Under Controlled Conditions. Protoplasma 1987; 136: 136-144.

Cámara B, De Los Ríos A, García-del-Cura MA, Galván V, Ascaso C. Dolostone bioreceptivity to fungal colonization. Materiales de Construcción 2008; 58: 113-124.

Cámara B, De los Ríos A, Urizal M, Álvarez de Buergo M, Varas MJ, Fort R, et al. Characterizing the Microbial Colonization of a Dolostone Quarry: Implications for Stone Biodeterioration and Response to Biocide Treatments. Microbial Ecology 2011; 62: 299-313.

Caneva G, Nugari MP, Salvadori O. Control of Biodeterioration and Bioremediation Techniques In: Caneva G, Nugari MP, Salvadori O, editors. Plant Biology for Cultural Heritage. Biodeterioration and Conservation. Getty Publications, Los Angeles, 2008, pp. 309-345.

Charola AE, McNamara C., R. K. Biocolonization of stone: control and preventive methods Smithsonian contributions to museum conservation Number 2. Smithsonian Institution Scholarly Press, Washington D.C., 2011, pp. 115.

De los Ríos A, Ascaso C. Preparative techniques for transmission electron microscopy and confocal laser scanning microscopy of lichens. In: Kranner I, Beckett RP, Varma AK, editors. Protocols in Lichenology. Springer, Berlin, 2002, pp. 87-151.

De los Ríos A, Ascaso C. Contributions of *in situ* microscopy to the current understanding of stone biodeterioration. International Microbiology 2005; 8: 181-188.

De los Ríos A, Cámara B, García del Cura MA, Rico VJ, Galván V, Ascaso C. Deteriorating effects of lichen and microbial colonization of carbonate building rocks in the Romanesque churches of Segovia (Spain). Science of The Total Environment 2009; 407: 1123-1134.

De los Ríos A, Galván V, Ascaso C. In situ microscopy diagnosis of biodeterioration processes occurring in the convent of Santa Cruz la Real (Segovia, Spain). International Biodeterioration & Biodegradation 2004; 54: 113-120.

De los Ríos A, Pérez-Ortega S, Wierzchos J, Ascaso C. Differential effects of biocide treatments on saxicolous communities: Case study of the Segovia cathedral cloister (Spain). International Biodeterioration & Biodegradation 2012; 67: 64-72.
Favero-Longo SE, Borghi A, Tretiach M, Piervittori R. In vitro receptivity of carbonate rocks to endolithic lichen-forming aposymbionts. Mycological Research 2009; 113: 1216-1227.
Gadd GM. Geomycology: biogeochemical transformations of rocks, minerals, metals and radionuclides by fungi, bioweathering and bioremediation Mycological Research 2007: 3-49.
Gorbushina AA, Broughton WJ. Microbiology of the Atmosphere-Rock Interface: How Biological Interactions and Physical Stresses Modulate a Sophisticated Microbial Ecosystem. Annual Review of Microbiology 2009; 63: 431-450.
Gorbushina AA, Diakumaku E, Müller L, Krumbein WE. Biocide treatment of rock and mural paintings: Problems of application, molecular techniques of control and environmental hazards. In: Saiz-Jimenez C, editor. Molecular Biology and Cultural Heritage. Swets & Zelinger Lisse, 2003.
Gueidan C, Thüs H, Pérez-Ortega S. Phylogenetic position of the brown algae-associated lichenized fungus *Verrucaria tavaresiae* (Verrucariaceae). Bryologist 2011; 114: 563-569.
Jensen M. Measurement of chlorophyll fluorescence in lichens. In: Kranner I. RBaAV, editor. Protocols in lichenology. Culturing, biochemistry, ecophysiology and use in biomonitoring. Springer, Berlin Heildelberg Nwe York, 2002.
Kappen L, Schroeter B, Green TGA, Seppelt RD. Chlorophyll *a* fluorescence and CO_2 exchange of *Umbilicaria aprina* under extreme light stress in the cold. Oecologia 1998; 113: 325-331.
Maxwell K, Johnson GN. Chlorophyll fluorescence-a practical guide. Journal of Experimental Botany 2000; 345 659-668.
Metz JG, Pakrasi HB, Seibert M, Arntzen CJ. Evidence for a dual function of the herbicide-binding D1 protein in photosystem II. FEBS Letters 1986; 205: 269-274.
Miller AZ, Sanmartín P, Pereira-Pardo L, Dionísio A, Saiz-Jimenez C, Macedo MF, et al. Bioreceptivity of building stones: A review. Science of the Total Environment 2012; 426: 1-12.
Nayaka S, Ranjan S, Saxena P, Pathre UV, Upreti DK, Singh R. Assessing the vitality of Himalayan lichens by measuring their photosynthetic performances using chlorophyll fluorescence technique. Current Science 2009; 97: 538-545.
Nimis PL, Martellos S. The Information System on Italian Lichens. In: Version 4.0. University of Trieste DoB, IN4.0/1. http://dbiodbs.univ.trieste.it/, editor, 2010.
Penh UP. International Coordinating Committee for the safeguarding and development of the historic site of AngkorTwelfth plenary session. In: UNESCO, editor. KH/CLT/2005/RP/10, 2008, pp. 187.
Rapsch S, Ascaso C. Effect of evernic acid on structure of spinach chloroplasts. Annals of Botany 1985; 56: 467-473.
Schroeter B, Green TGA, Seppelt RD, Kappen L. Monitoring photosynthetic Activity of crustose lichens using a PAM-2000 Fluorescence System. Oecologia 1992; 92: 457-462.
Schroeter B, Sancho LG, Valladares F. *In situ* comparison of daily photosynthetic activity patterns of saxicolous lichens and mosses in Sierra de Guadarrama, Central Spain. The Bryologist 1999; 102: 623-633.
Smith CW, Aptroot A, Coppins BJ, Fletcher A, Gilbert OL, James PW, et al. The lichens of Great Britain and Ireland. London: British Lichen Society 2010.
Smithsonian I. A Survey of the Rock Substrates of Petroglyphs at Gobustan, Azerbaijan. In: Program SIACH, editor. Smithsonian Institution, Washington, D.C, 2012, pp. 55.
Speranza M, Sanz M, Oujja M, de los Rios A, Wierzchos J, Pérez- Ortega S, et al. ND:YAG Laser irradiations damage to endolithic and epilithic microorganisms. International Biodegradation & Biodeterioration 2012; in press.

Tretiach M, Bertuzzi S, Salvadori O. Chlorophyll a fluorescence as a practical tool for checking the effects of biocide treatments on endolithic lichens. International Biodeterioration & Biodegradation 2010; 64: 452-460.
Tretiach M, Crisafulli P, Imai N, Kashiwadani H, Heemoon K, Wada H, et al. Efficacy of a biocide tested on selected lichens and its effects on their substrata. International Biodeterioration & Biodegradation 2007; 59: 44-54.
Uchida E, Ogawa Y, Maeda N, Nakagawa T. Deterioration of stone materials in the Angkor monuments, Cambodia. Engineering Geology 2000; 55: 101-112.
Wierzchos J, Ascaso C. Application of back-scattered electron imaging to the study of the lichen-rock interface. Journal of Microscopy 1994; 175: 54-59.

Figure 1. General view of the Redueña dolostone quarry, *Verrucaria nigrescens* colonisation and microclimate data.

Quarry face (A) occupied by the *Verrucaria nigrescens* thalli (open white arrows in B) and the grid placed in experimental plots (inset in B) to identify each lichen thallus during the assessment of the biocide effect on lichen photosynthetic performance. Microclimate data (C), relative air humidity (RH) and air temperature (T), from both of the previous days and during the experiment. Black arrows indicate the start of the experiment.

Figure 2. Fv/Fm measured in the field in thalli of *Verrucaria nigrescens* control and after and before treatment with Koretrel (1.5 and 3 % water dilutions). Both curves show values of Fv/Fm = 0.520 at time 0. N = 51, 92 and 117 for control, Koretrel 1.5% and Koretrel 3% water dilutions, respectively; error bars represent standard deviations (SD).

Figure 3. SEM-BSE images of *Verrucaria nigrescens* epilithic thalli (A-D) and a cluster of microbial endolithic colonisation (D) of dolomite stone without biocide treatment (control plot). *V. nigrescens* epilithic thalli (open white arrows in A and D). Upper cortex (white arrow in B), photobiont layer (solid white arrows in B), photobiont (solid white arrow in C) and mycobiont hyphae (solid black arrows in B and C) with strong signals produced by the OsO_4 staining of cytoplasmatic lipids in vital lichen thalli. Lichen medullar region (dotted black arrows in B).

Minerals trapped and microdivided (black asterisks in B) between the lichen thalli. Clusters of microorganisms (black arrows and inset), fungi (solid black arrows in inset) and algae (solid white arrows in inset) localised in endolithic zones.

Figure 4. SEM-BSE images of *Verrucaria nigrescens* epilithic thalli after 28 days of treatment with the 1.5% Koretrel solution. General view (A) and details (B-D) of the biocide effect on lichen thalli (open white arrows in A, B and D. Detailed view (C) of the algal cells with plasmolysis (white solid arrows) and fungal hyphae (black solid arrows) showing only the cell wall. Note the strong signals produced by the OsO_4 staining of cytoplasmatic lipids in some fungal hyphae (white dotted arrows in D) in lichen thalli after biocide.

Figure 5. TEM images showing the ultrastructural appearance of the photobiont of *Verrucaria nigrescens* control (A) and after the application of 1.5 % Koretrel solution (B). The normal appearance of the chloroplasts (ch) of the algae (A), the thylakoid lamellae (t), the pyrenoid (p) (Fig. 5A), and an adjacent fungal hyphae (H) could be distinguished. The chloroplasts (ch) and the thylakoids structure have disappeared (∗), and the pyrenoglobuli are difficult to distinguish (p) after biocide treatment (Fig. 5B). Mass formed by thylakoid lipid remains.

Figure 6. SEM-BSE images of the effects of the 3% Koretrel solution after 28 days of treatment. The biocide action could be observed in all lichen thalli (open white arrows in A and details in B-C). Note the fungal endolithic colonisation and the important changes in the dolostone in the basal zone of the lichen thalli (white circle in B) and in the deeper endolithic zone (black inset in A). The photobiont layer (solid white arrows in C) and mycobiont hyphae (solid black arrows in C) showing evident morphological damage such as plasmolysis produced by the biocide

treatment. A detail view (D) of the black inset from A showing fungal hyphae (black dotted arrows) without lipid body signals.

Figure 7. Macroscopic and microscopic images before (A) and after (B-D) mechanical cleaning of lichen thalli treated with the 3% Koretrel solution.

Verrucaria nigrescens black crustose thalli on dolostone quarry face (A). Green discoloration of the dolostone surface after lichen thalli removal (B). Endolithic clusters formed by phototrophic and heterotrophic microorganisms are localised near the stone surface. Some clusters (black arrow in C) and cells (black arrow inside the inset in C) show normal morphology, and others present a damaged aspect (white arrow in C). Alga (white arrow in D) and fungi (black arrow in D) did appear not to be affected by the biocide; note the intense BSE signal emitted by the fungal lipid bodies (black solid arrows in C and D).

Figure 1

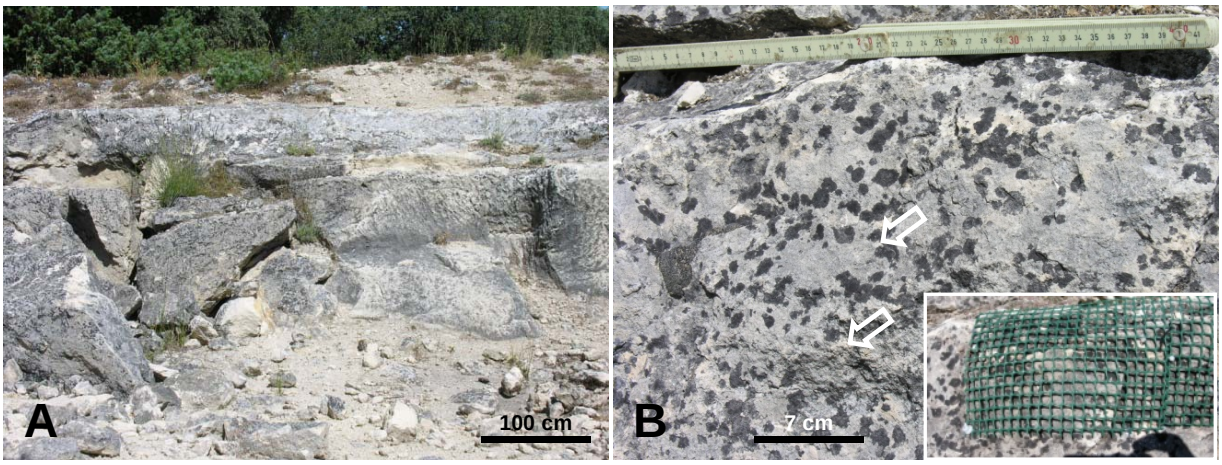
A
100 cm
B
7 cm

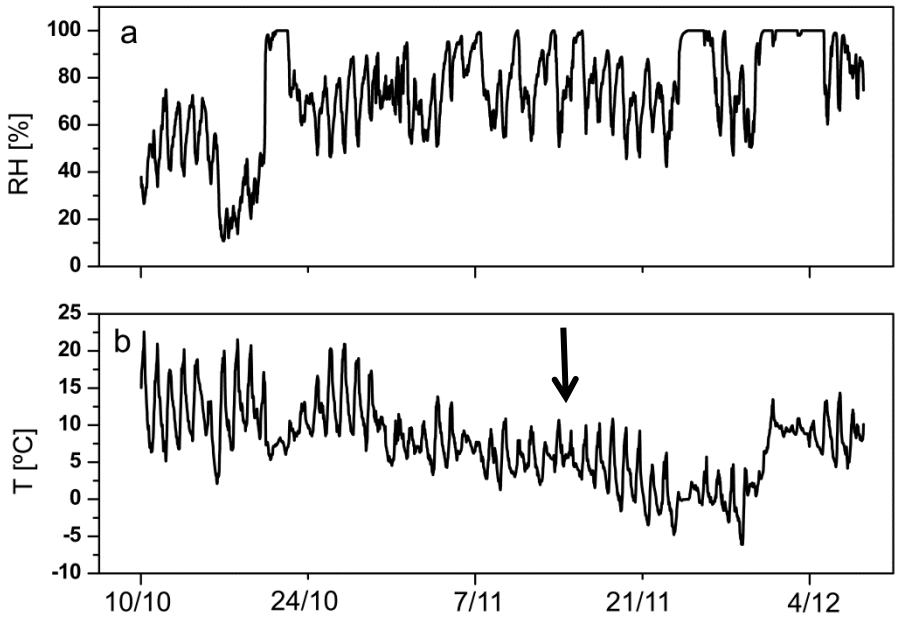
a
RH [%]
100
80
60
40
20
0
b
T [ºC]
25
20
15
10
5
0
-5
-10
10/10
24/10
7/11
21/11
4/12

E

Figure 2

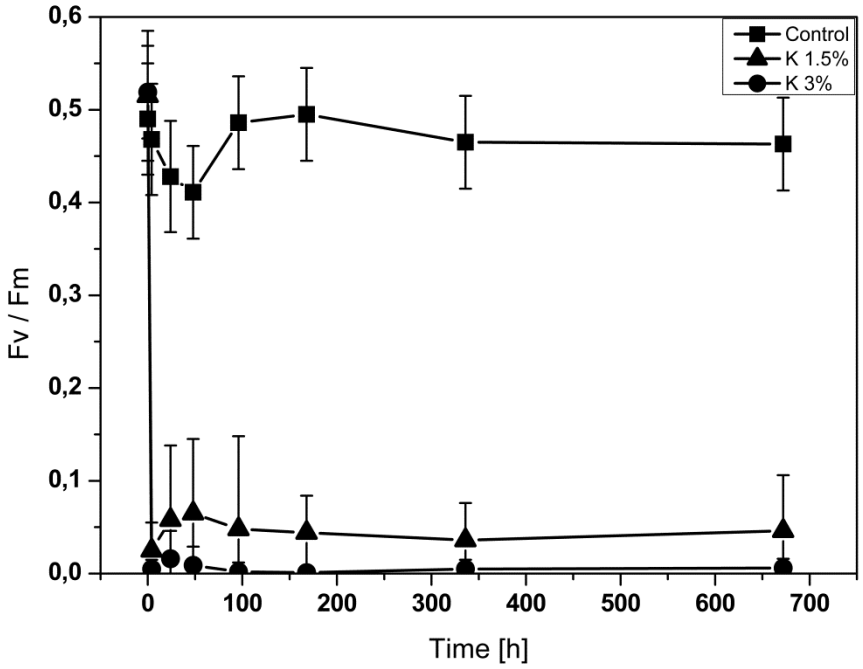
Control
K 1.5%
K 3%
Fv / Fm
0,0
0,1
0,2
0,3
0,4
0,5
0,6
0
100
200
300
400
500
600
700
Time [h]

Figure 3

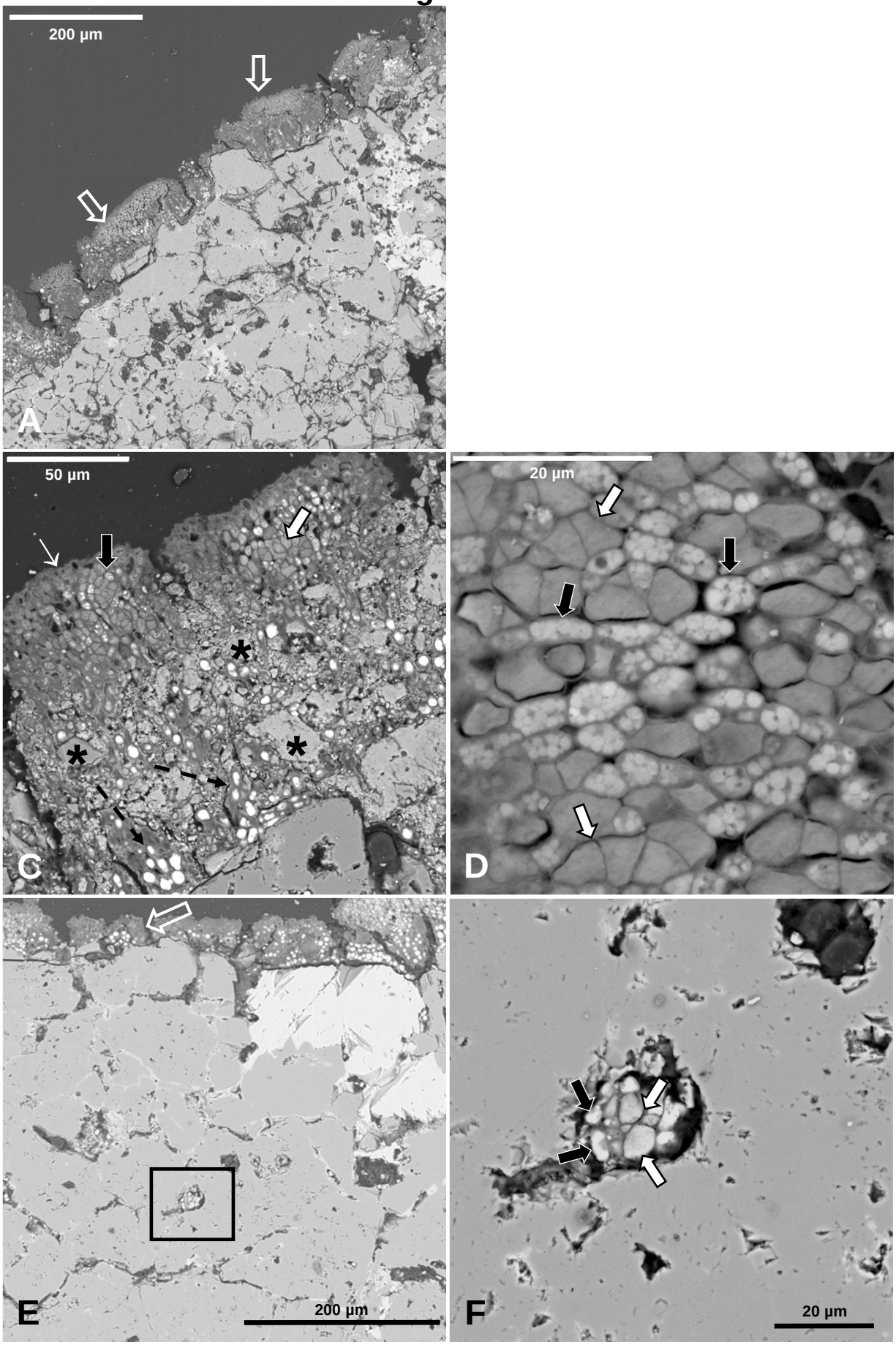

Figure 4

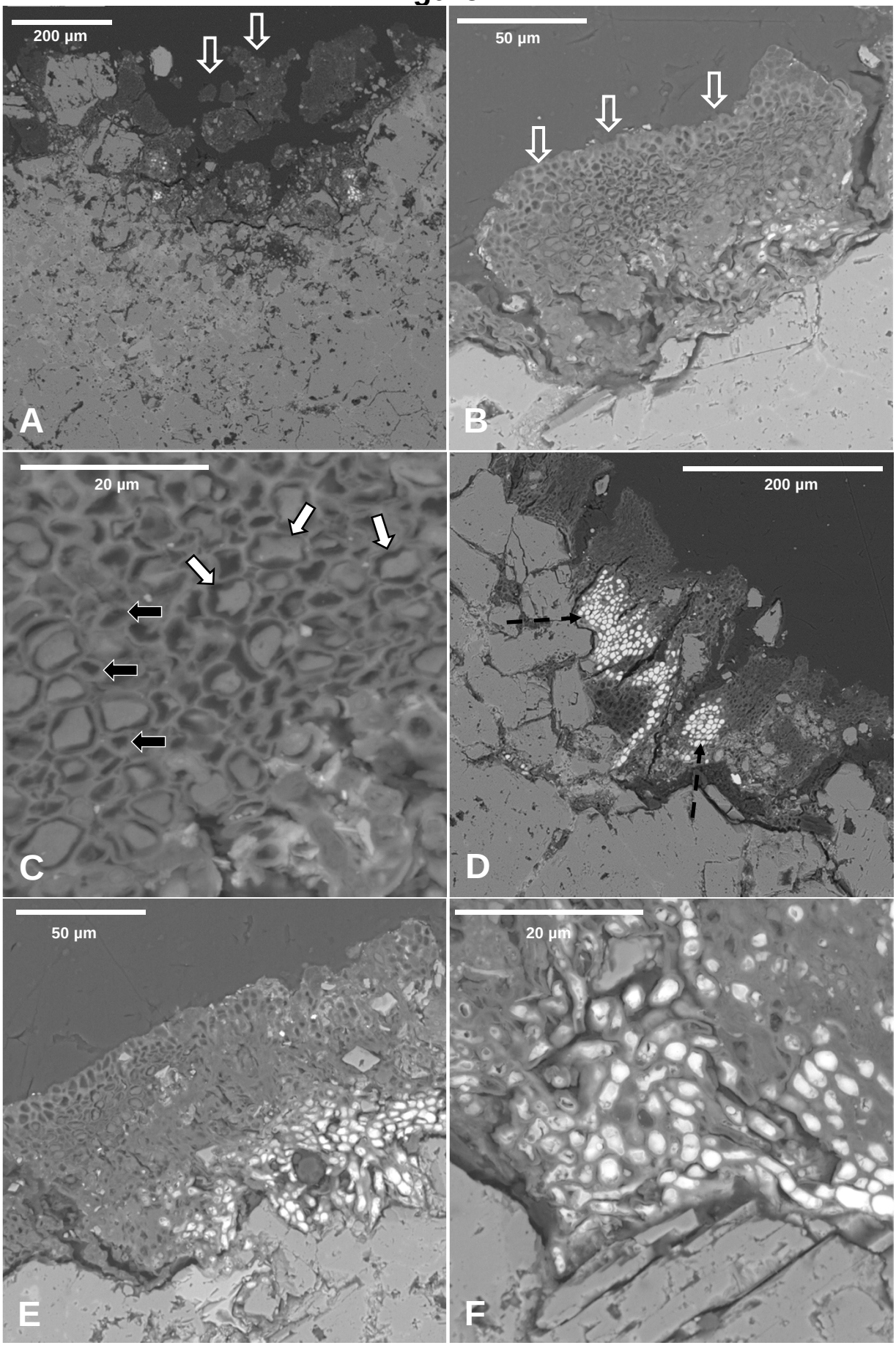

Figure 5

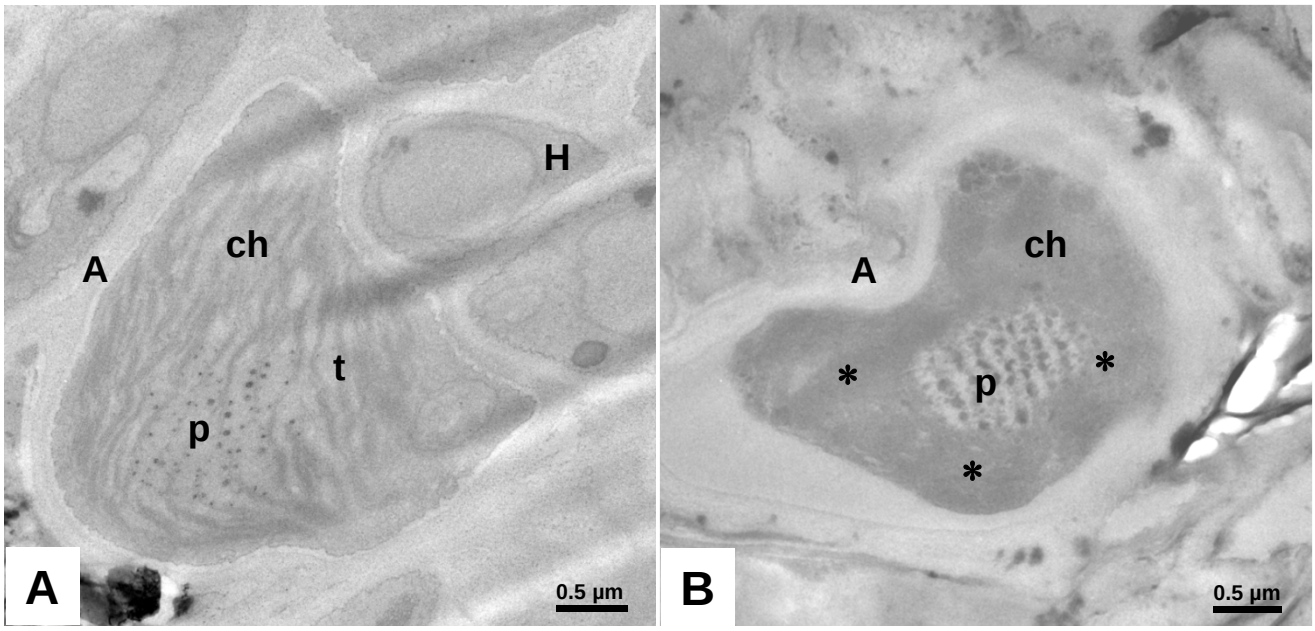

Figure 6

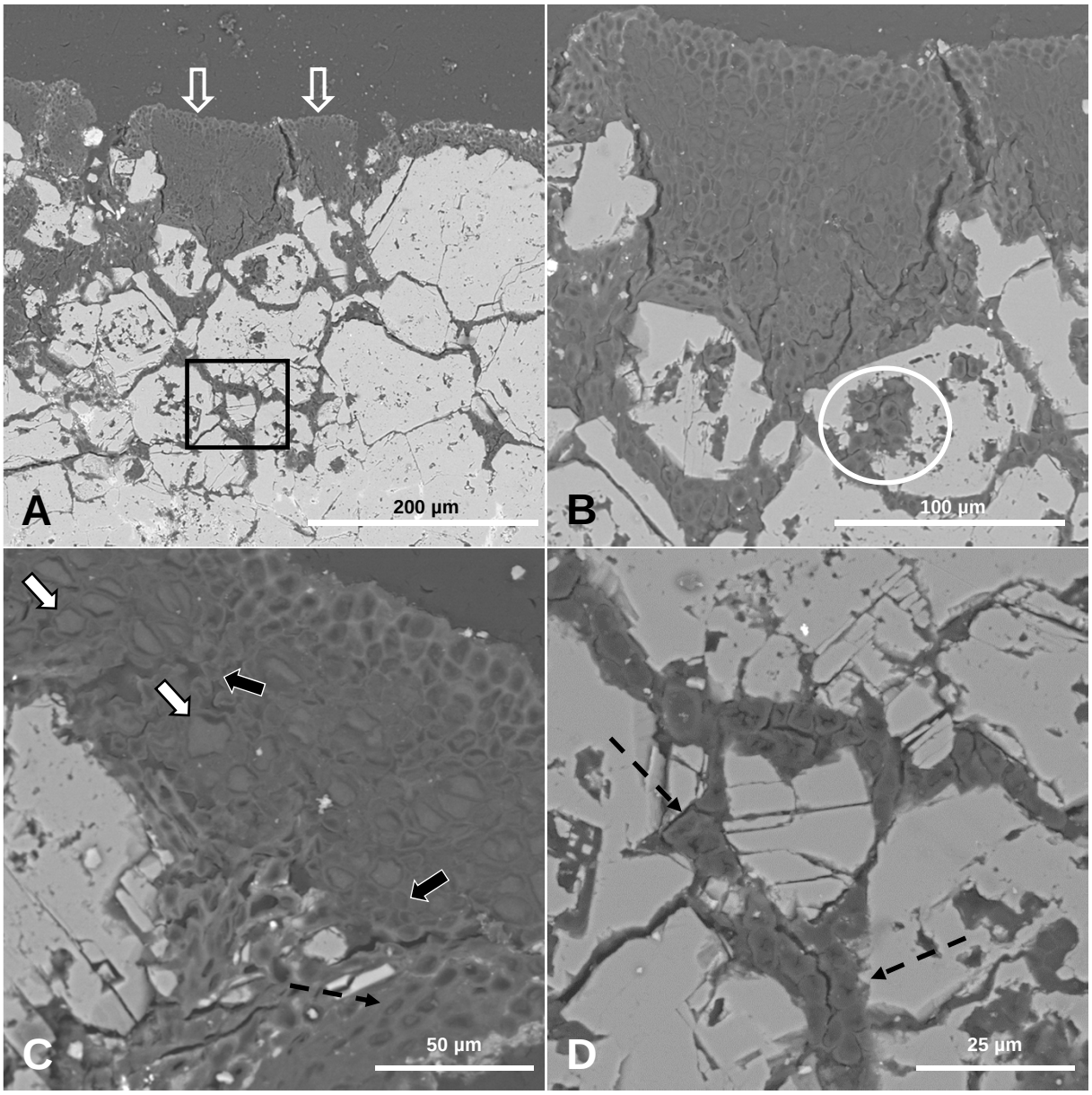

Figure 7

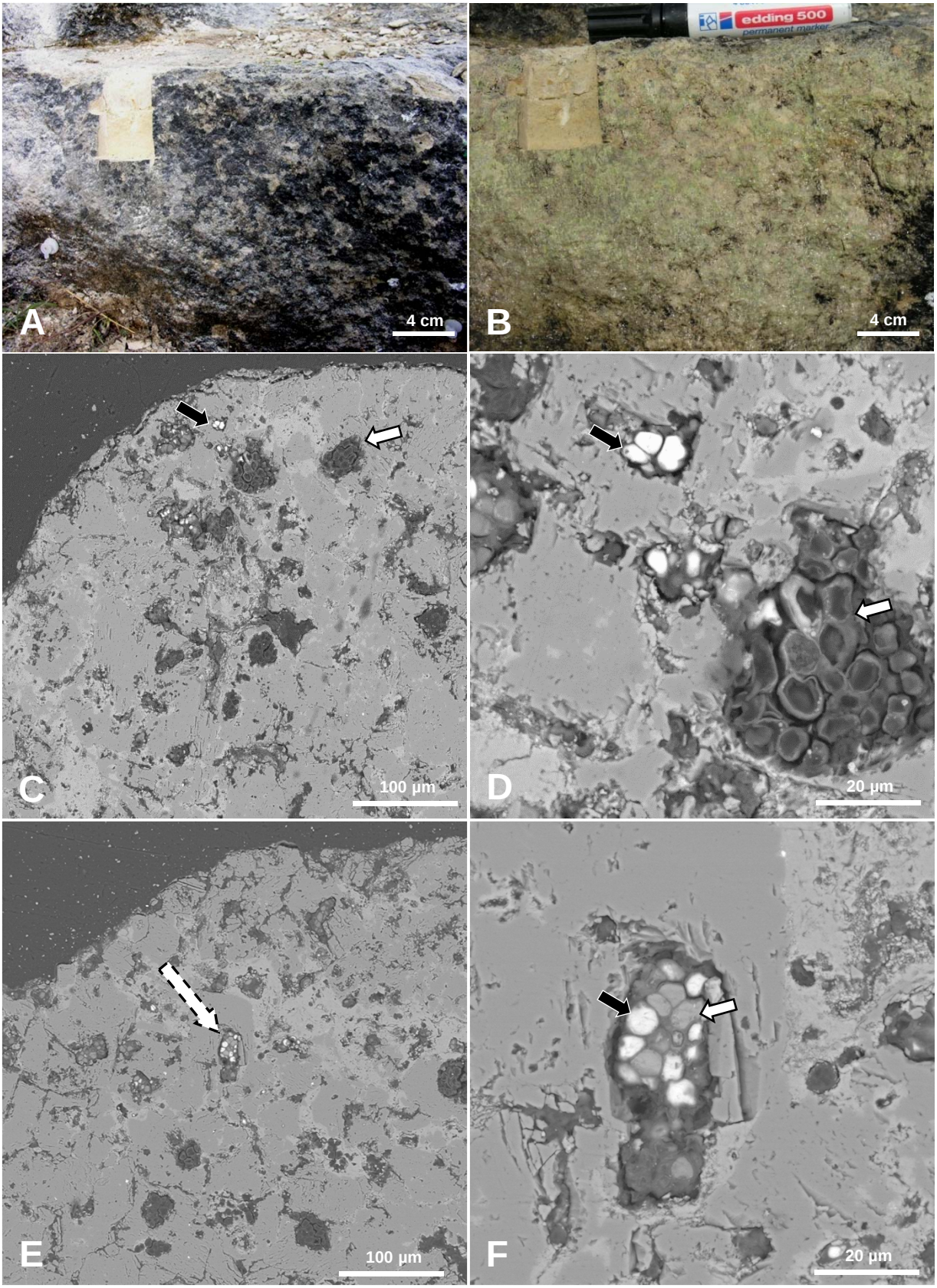
A
4 cm
B
edding 500
permanent marker
4 cm
C
100 µm
D
20 µm
E
100 µm
F
20 µm